






# Global Phylogeography of Marine *Synechococcus* in Coastal Areas Reveals Strong Community Shifts

 Hugo Doré,<sup>a\*</sup> Jade Leconte,<sup>a</sup> Ulysse Guyet,<sup>a§</sup> Solène Breton,<sup>a</sup> Gregory K. Farrant,<sup>a</sup> David Demory,<sup>a</sup>  Morgane Ratin,<sup>a</sup> Mark Hoebeke,<sup>b</sup> Erwan Corre,<sup>b</sup> Frances D. Pitt,<sup>c∞</sup> Martin Ostrowski,<sup>c‡</sup> David J. Scanlan,<sup>c</sup> Frédéric Partensky,<sup>a</sup> Christophe Six,<sup>a</sup>  Laurence Garczarek<sup>a</sup>

<sup>a</sup>Sorbonne Université, CNRS, UMR 7144 Adaptation and Diversity in the Marine Environment (AD2M), Station Biologique de Roscoff (SBR), Roscoff, France

<sup>b</sup>CNRS, FR 2424, ABiMS Platform, Station Biologique, Roscoff, France

<sup>c</sup>University of Warwick, School of Life Sciences, Coventry, United Kingdom

**ABSTRACT** Marine *Synechococcus* comprise a numerically and ecologically prominent phytoplankton group, playing a major role in both carbon cycling and trophic networks in all oceanic regions except in the polar oceans. Despite their high abundance in coastal areas, our knowledge of *Synechococcus* communities in these environments is based on only a few local studies. Here, we use the global metagenome data set of the Ocean Sampling Day (June 21<sup>st</sup>, 2014) to get a snapshot of the taxonomic composition of coastal *Synechococcus* communities worldwide, by recruitment on a reference database of 141 picocyanobacterial genomes, representative of the whole *Prochlorococcus*, *Synechococcus*, and *Cyanobium* diversity. This allowed us to unravel drastic community shifts over small to medium scale gradients of environmental factors, in particular along European coasts. The combined analysis of the phylogeography of natural populations and the thermophysiological characterization of eight strains, representative of the four major *Synechococcus* lineages (clades I to IV), also brought novel insights about the differential niche partitioning of clades I and IV, which most often co-dominate the *Synechococcus* community in cold and temperate coastal areas. Altogether, this study reveals several important characteristics and specificities of the coastal communities of *Synechococcus* worldwide.

**IMPORTANCE** *Synechococcus* is the second most abundant phytoplanktonic organism on Earth, and its wide genetic diversity allowed it to colonize all the oceans except for polar waters, with different clades colonizing distinct oceanic niches. In recent years, the use of global metagenomics data sets has greatly improved our knowledge of “who is where” by describing the distribution of *Synechococcus* clades or ecotypes in the open ocean. However, little is known about the global distribution of *Synechococcus* ecotypes in coastal areas, where *Synechococcus* is often the dominant phytoplanktonic organism. Here, we leverage the global Ocean Sampling Day metagenomics data set to describe *Synechococcus* community composition in coastal areas worldwide, revealing striking community shifts, in particular along the coasts of Europe. As temperature appears as an important driver of the community composition, we also characterize the thermal preferenda of 8 *Synechococcus* strains, bringing new insights into the adaptation to temperature of the dominant *Synechococcus* clades.

**KEYWORDS** marine cyanobacteria, *Synechococcus*, coastal areas, Ocean Sampling Day, temperature, niche partitioning, metagenomics

**B**etter assessment of the spatial and temporal variability of the genetic diversity, structure, and dynamics of marine phytoplankton communities is critical to predicting their future evolution in environments whose physicochemical properties are continuously altered by the ongoing global change. The marine picocyanobacteria

**Editor** Jeffrey Lawrence Blanchard, University of Massachusetts Amherst

**Copyright** © 2022 Doré et al. This is an open-access article distributed under the terms of the [Creative Commons Attribution 4.0 International license](https://creativecommons.org/licenses/by/4.0/).

Address correspondence to Laurence Garczarek, [laurence.garczarek@sb-roscoff.fr](mailto:laurence.garczarek@sb-roscoff.fr).

\*Present address: Hugo Doré, Université de Brest - UMR BEEP CNRS/UBO/Ifremer - IUEM, Rue Dumont D'Urville, Plouzané, France.

§Present address: Ulysse Guyet, Université de Bordeaux, CNRS, IBGC, UMR 5095, Bordeaux, France.

◇Present address: David Demory, School of Biological Sciences, Georgia Institute of Technology, Atlanta, Georgia, USA.

∞Present address: Frances D. Pitt Rosalind, Franklin Laboratory, Leamington Spa, United Kingdom.

‡Present address: Martin Ostrowski, Climate Change Cluster, University of Technology, Broadway, New South Wales, Australia.

The authors declare no conflict of interest.

**Received** 15 July 2022

**Accepted** 11 November 2022

**Published** 5 December 2022

*Prochlorococcus* and *Synechococcus*, together accounting for about 25% of ocean net primary production (1), are key members of phytoplankton communities and constitute particularly relevant models to tackle this issue. *Prochlorococcus* distribution is restricted to the 45°S to 50°N latitudinal band, this organism preferentially thriving in oligotrophic areas, while *Synechococcus* is present in all marine environments from the equator to subpolar waters but reaches its highest abundances in nutrient-rich areas (2–8).

The ability of these 2 genera to colonize a wide range of ecological niches is likely related to their large genetic diversity (9–13). For *Prochlorococcus*, numerous environmental and laboratory studies have revealed the clear-cut niche partitioning between physiologically and genetically distinct ecotypes, with ‘phototypes’ (14), ‘thermotypes’ (3, 15, 16), and ‘nutritypes’ (12, 17, 18), occupying distinct light, thermal and nutrient (+Fe/- Fe) niches. Besides *Prochlorococcus*, ‘Cluster 5’ *sensu* Herdman et al. (19) also encompasses 3 major *Synechococcus/Cyanobium* lineages, called sub-clusters (SC) 5.1 through 5.3 (9, 20). Although a number of phylogenetic studies based on individual markers have considered SC 5.2 and *Cyanobium* as being 2 distinct lineages (21–23), the delineation is unclear and it was recently proposed, based on comparative genomics, that all members of these lineages should be gathered into a single group (SC 5.2) named ‘*Cyanobium*’, even though the level of genomic diversity within this group is quite large (20, 24, 25). SC 5.2 gathers freshwater and halotolerant representatives and thus in the marine environment, members of this group are only found in significant abundance in river-influenced coastal waters, such as the Chesapeake Bay (21, 22, 26) or the Pearl River estuary (27, 28), and in low salinity areas such as the Baltic Sea (29). SC 5.3 was long thought to contain only obligatory marine representatives and was shown to account for a significant fraction of the *Synechococcus* community in some specific marine areas, including the Mediterranean Sea and northwestern Atlantic Ocean (12, 30–32). However, freshwater members of this group were recently discovered in the Tous reservoir (Spain) and were then found to be broadly distributed in temperate freshwater lakes (25, 33). Finally, SC 5.1, a lineage that rapidly diversified after the advent of the *Prochlorococcus* radiation (34, 35), is by far the most widespread and abundant *Synechococcus* lineage in the open ocean environment, e.g., representing more than 93% of total *Tara* Oceans metagenomic reads assigned to SC 5.1 to 5.3 (12). From 10 to 15 phylogenetic clades have been defined within SC 5.1 depending on the phylogenetic marker (10, 30, 36) but studies of the global distribution patterns of *Synechococcus* populations in open ocean waters have shown that there are 5 major clades *in situ* (I, II, III, IV, and CRD1), with clades I and IV co-dominating *Synechococcus* communities in cold and temperate, nutrient-rich areas, while clades II, III, and CRD1 preferentially thrive in warm waters (5, 12, 31, 32, 37, 38).

Physiological measurement of temperature preferences of strains belonging to clades I, II, III, IV, and V isolated across different latitudes further confirmed the existence of warm (clades II, III, V) and cold (clades I and IV) ‘thermotypes’ (38–42). Despite being phylogenetically distant, clades I and IV were further demonstrated to share a number of physiological adaptations to cold water, including a higher thermal sensitivity of phycobiliproteins (43), a similar change in membrane lipids (40, 44) and an increase of the photoprotection capacities using the orange carotenoid protein (OCP; 45). Nutrients were also found to play a key role in structuring these populations, with clade II, the most abundant *Synechococcus* lineage in the ocean, dominating the *Synechococcus* community in N-poor areas, clade III in P-poor areas, while CRD1 is restricted to Fe-depleted waters (5, 12, 32, 37).

Although the variability of picocyanobacterial communities and the main physicochemical factors driving their composition are starting to be well understood in open ocean environments, the picture is much more fragmentary in coastal areas. Indeed, most coastal studies have concerned specific regions, such as the Baltic Sea, the Californian coast or estuarine waters (e.g., the Chesapeake Bay or coastal waters of Hong Kong; [21–23, 26, 28, 29, 45]) and/or a few long-term monitoring sites of coastal

observatories (24, 46–50). Here, in order to get a more global view of the genetic diversity and biogeography of coastal populations of picocyanobacteria and to better understand how they vary between distinct coastal areas and differ from open ocean populations, we used metagenomic data from the Ocean Sampling Day (OSD) 2014 campaign (51), encompassing 157 coastal samples collected all over the world at the summer solstice, employing the same protocol for collecting DNA samples and associated metadata. Using a whole genome recruitment (WGR) approach, we assessed the genetic diversity and the clade level composition of *Synechococcus* communities in OSD samples. Given the previously recognized role of temperature in structuring *Synechococcus* communities, we then analyzed the distribution patterns of the different lineages in light of previously published and new comparative thermophysiological data on *Synechococcus* strains representative of the most abundant clades in the field. The excellent spatial resolution achieved in northern Atlantic and Mediterranean coastal waters allowed us to observe several spatial community shifts and to enlighten the roles of temperature and salinity as key drivers of coastal *Synechococcus* community composition.

## RESULTS AND DISCUSSION

**Biogeography of coastal picocyanobacterial communities is influenced by seawater temperature.** Most of the stations sampled during the OSD 2014 campaign (51) correspond to coastal areas with only 17 of 157 stations located over 11 nautical miles from the nearest coast. This data set displays a particularly good spatial resolution in some regions of the world ocean and notably along European and Eastern United States coasts, while only a few of the sampled sites were located in the Southern Hemisphere (7 out of 157) (Fig. S1). Here, we used the 150 metagenomes obtained in the framework of this campaign, altogether totaling 41 Gbp (168.7 million reads), to assess the relative abundance of *Synechococcus/Cyanobium* and *Prochlorococcus* clades. *Prochlorococcus* was only abundant at a few stations, likely due to the coastal localization of the sampling sites, and was therefore not included in subsequent analyses. By contrast, *Synechococcus/Cyanobium*, known to largely outnumber *Prochlorococcus* in coastal areas (2, 7, 24, 52), was detected with sufficient coverage to perform reliable taxonomic assignment at the clade level in 102 out of the 150 OSD metagenomes, using a conservative lowest common ancestor approach for taxonomic assignment (see Materials and Methods). At most stations, the *Synechococcus/Cyanobium* community was dominated by 1 or 2 taxa among SC 5.1 clades I–IV, SC 5.2 or SC 5.3 (Fig. 1). Consistent with previous studies on the picocyanobacterial distribution in open ocean waters (6, 12, 15, 30, 32, 37), clades I and IV dominated at latitudes above 35°N (except in the Mediterranean Sea) and clade II at latitudes below 35°N, while clade III was almost exclusively present and often dominant in the Mediterranean Sea. It is also worth noting that the co-occurrence of clades I and IV at the few stations beyond 35°S in the Southern hemisphere mirrored the profiles obtained at the same latitude in the Northern hemisphere, which is in agreement with previous observations in open ocean waters (12, 30, 32, 37), as well as with the low temperatures of isolation sites of clade I and IV strains (39).

To further explore the role of temperature on the differential latitudinal distribution of members of clades I to IV, we characterized the thermal referenda of 8 strains belonging to these clades (Table 1, Fig. 2). While several strains belonging to clade I were previously shown to withstand colder temperatures than their tropical clade II counterparts (38–40, 53), growth optima and boundary limits for temperature were only available for 1 clade IV (38, 40, 42) and 2 closely related clade III strains (38, 40, 41, 54), and results were obtained in different light conditions, making them difficult to compare. Here, the direct comparison of clades I and IV strains, grown under the same conditions, showed quite similar thermal preferences. All tested strains of these 2 clades displayed an optimal temperature for growth of about 24°C according to our model fit (Fig. 2 and Table 2), and were able to grow at the lowest tested temperature, 10°C, which is also the lowest temperature measured in the OSD 2014 stations where the *Synechococcus* community was analyzed. In comparison, clades II and III strains

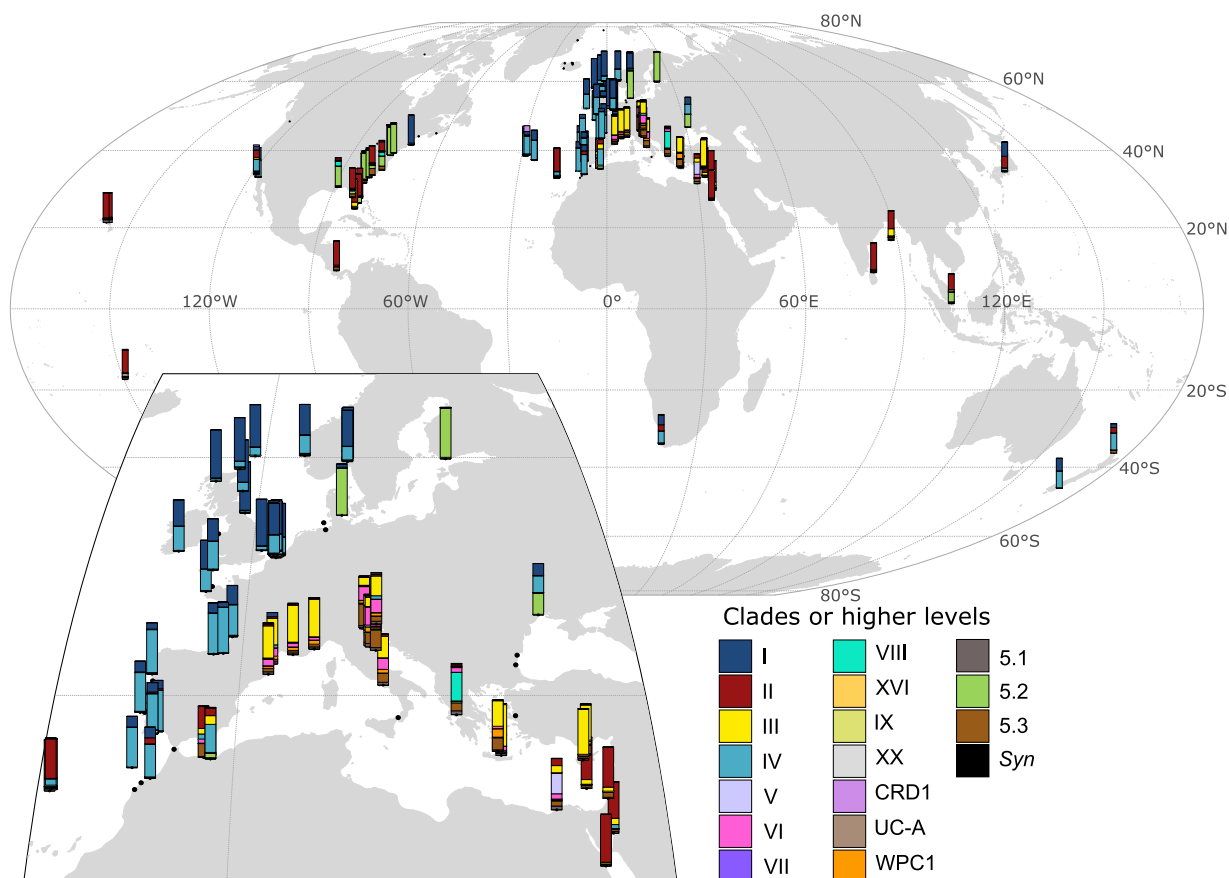


**FIG 1** Relative abundance of marine *Synechococcus* clades in Ocean Sampling Day stations. Stations are located at the bottom of barplots of relative abundance. The insert shows a closeup version of Europe. Station numbers are shown in Fig. S1. Categories 5.1 and *Syn* correspond to reads that could not be assigned to a clade but were assigned to the higher taxonomic levels of *Synechococcus* SC 5.1 or *Synechococcus* genus, respectively.

were not able to grow at temperatures of 13°C and below, thus confirming with several strains that clades I and IV are cold thermotypes, whereas clades II and III are warm thermotypes. Altogether, these results support the idea that differences in thermophysiology at least partially explain the latitudinal distribution of these 4 clades.

Besides the abundance of clades I and IV, coastal *Synechococcus* communities also exhibited some other specificities compared to open ocean populations, notably the very low relative abundance of clade CRD1, which was shown to be prevalent in large regions of the open ocean that are limited by iron availability (12, 32, 37), as well as the dominance of SC 5.2 in the brackish Baltic sea and at stations along the Atlantic coast of North America, often co-occurring with a low proportion of clade VIII. The latter observation is most likely due to the influence of riverine inputs at these OSD stations, these taxa being known to occur in estuarine areas and to contain strains growing over a large range of salinity (9, 21, 36). This hypothesis was further confirmed by clustering stations according to the relative abundance profiles of *Synechococcus* clades (Fig. 3), which clearly separated stations dominated by subcluster 5.2 and showed that they had a lower salinity than most other stations (Fig. 4B, cluster 5). Finally, clades V and VI, which were not distinguished from clade VII (and CRD1) in previous global surveys of *Synechococcus* distribution using the low-resolution 16S rRNA marker gene, were found to be locally abundant in the data set. While the V/VI/VII/CRD1 group was considered to be widely distributed in oceanic waters (15, 30, 55), our analysis reveals the potential preference for coastal areas of the closely related clades V and VI. This result is consistent with the previous local observations of the occurrence of clade V-

**TABLE 1** Information regarding the *Synechococcus* strains used in this study

Strain name	CC9311	ROS8604	M16.1	PROS-U-1	RS9915	A15-28	MVIR-16-1	MVIR-11-1
RCC no.	1086	2380	791	2369	2553	2556	2570	1695
Clade	I (Ia)	I (Ib)	II (IIa)	II (IIh)	III (IIIa)	III (IIIb)	IV (IVa)	IV (IVa)
Pigment type <sup>a</sup>	3dA	3a	3a	3dB	3dB	3c	3d	3a
Isolation site	California Current	English Channel	Gulf of Mexico	Moroccan upwelling	Red Sea - Gulf of Aqaba	Atlantic Ocean Northern gyre	North Sea	North Sea
Isolation latitude	32° 0' N	48° 43' N	27° 42' N	30° 8' N	29° 28' N	31° 15' N	60° 19' N	56° 56' N
Isolation longitude	124° 31' W	3° 59' W	91° 18' W	10° 3' W	34° 55' E	20° 43' W	3° 29' W	3° 59' E
Isolation date	01/01/93	11/24/86	02/09/04	09/12/99	10/18/99	09/25/04	07/21/07	01/14/07
Isolation depth (m)	95	1	275	5	10	15	10	10
Isolation temp. (°C) <sup>b</sup>	16.59	12.81	24.15	21.51	23.98	25.15	11.99	15.09
Coast distance (km)	458	0.5	156	35	3	369	78	201

<sup>a</sup>The pigment type nomenclature is described in Humily et al. (2014).

<sup>b</sup>Isolation temperatures were retrieved from National Oceanic and Atmospheric Administration (NOAA) as described in Pittera et al. (2014).

and VI-related sequences at some coastal sites in the Adriatic Sea and the Pearl River Estuary (23, 49, 56).

**A progressive latitudinal shift in *Synechococcus*/*Cyanobium* communities along the coast of Europe.** Besides the above-mentioned specificities of coastal regions in terms of *Synechococcus*/*Cyanobium* community composition, we also observed changes in communities at a finer spatial scale along European coasts, where the OSD sampling effort was the highest (see zoom in Fig. 1 and Fig. S1 for station numbers). While along the southern part of this latitudinal gradient from the Moroccan to French Atlantic coasts, *Synechococcus* communities were dominated by clade IV, a clear progressive northward shift was observed toward the dominance of clade I in the North Sea (Fig. 1). Clustering of stations based on clade relative abundance indeed highlighted 2 groups of stations; the first one dominated by clade IV (Fig. 3, cluster 3) and the second one by clade I (Fig. 4B, cluster 4). Interestingly, clade I was found to dominate at stations that display a significantly lower salinity than those dominated by clades II or III (Fig. 3, clusters 1 and 2). These clade I-dominated stations also exhibited a significantly lower temperature (average 16.6°C, median 17°C) than all other clusters except cluster 3 dominated by clade IV (average temperature 19.1°C, median 19°C), the latter cluster of stations showing a significant difference in temperature only with cluster 2 (dominated by clade II). Thus, despite a clear latitudinal shift in the ratio of clade I to clade IV along the European coast, neither the difference in salinity nor the difference in seawater temperature seem to be sufficient to fully explain the observed changes.

Several potential reasons have been evoked to explain the variations in the clade I to clade IV ratio across space or time in coastal areas (46, 48, 57). These include differences in their respective adaptation to metal and/or nitrate concentrations (32, 46, 50), as well as transport and mixing of populations by advection, e.g., in the vicinity of the Svalbard island, where the Gulf Stream current brings clade IV populations in summer (4) or in the Korean Sea where the warm, oligotrophic Kuroshio Current was suggested to be responsible for the co-occurrence of clades I, II, and IV populations (58). Clade I was also suggested to be more coastal and opportunistic than clade IV (9, 46) but this hypothesis is not confirmed by this study since many coastal stations (cluster 3) are actually dominated by clade IV. Finally, this northward shift could also rely on differences occurring at a finer taxonomic level since several studies pointed out to the existence of several genotypes within clades I and/or IV, the relative abundance of which varies according to depth, latitude, phage interactions, season, or over the course of a bloom (4, 6, 27, 48, 50, 57, 59–61). In particular, coastal time series showed that different genotypes within clade I and/or IV follow distinct seasonal patterns, suggesting a

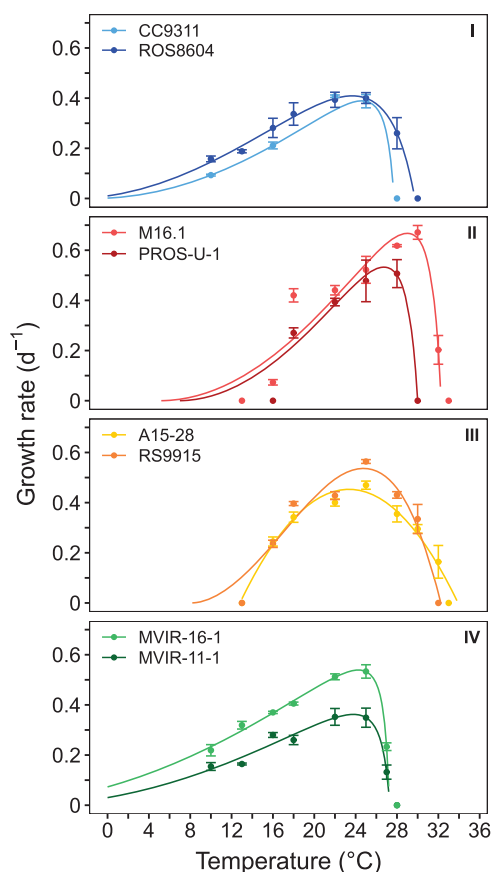


**FIG 2** Temperature preferenda of 8 marine *Synechococcus* strains. Growth rate as a function of temperature of acclimated growth. Two strains were chosen within each of the 4 major clades I, II, III, and IV (top to bottom). All cultures were grown at a light intensity of  $20 \mu\text{mol quanta m}^{-2} \text{s}^{-1}$ . Error bars are standard deviation from the mean based on at least 3 replicates ( $n \geq 3$ ). The line represents the best fit of the Cardinal Temperature Model with Inflection (BR model; 86).

differential adaptation of these genotypes to water temperature or other environmental parameters (48, 50, 60, 62).

Consistently, comparison of our experimental data with previous data acquired under the same light conditions (40) brings evidence that clade IV is comprised of distinct genotypes exhibiting different lower temperature boundary limits and, thus, potentially colonizing different thermal niches, as was also shown for clade I strains (39). Indeed, the 2 clade IV strains characterized here were sampled at high latitude (Table 1), and show a higher tolerance to cold temperatures than BL107, another clade

**TABLE 2** Parameters of growth versus temperature for 8 *Synechococcus* strains representative of the four most abundant clades

Clade	Strain	$T_{\text{opt}}^a$ measured <sup>b</sup>	$T_{\text{opt}}$ model <sup>c</sup>	$T_{\text{opt}}$ range <sup>d</sup>	$T_{\text{max}}^e$ measured <sup>b</sup>	$T_{\text{max}}$ model <sup>c</sup>	$T_{\text{max}}$ range <sup>d</sup>
I	CC9311	22	24.6	22.98–25.91	25	27.7	26.23–28.97
	ROS8604	25	23.7	22.23–24.80	28	29.7	28.19–31.36
IV	MVIR-16-1	25	24.3	23.37–25.09	27	27.3	27.06–27.47
	MVIR-11-1	22	23.8	22.42–25.05	27	27.3	26.93–27.63
III	RS9915	25	24.8	23.11–28.44	32	32.2	25.37–34.88
	A15-28	25	23.4	22.97–23.72	32	33.9	32.79–34.82
II	M16.1	30	29.0	27.99–30.19	32	32.3	31.93–32.51
	PROS-U-1	28	26.8	25.58–27.96	28	30.0	3.04–39.90

<sup>a</sup> $T_{\text{opt}}$ , optimal temperature for growth.

<sup>b</sup>Measured values, see Fig. 3.

<sup>c</sup>Values estimated by a model of growth versus temperature fitted to the data shown in Fig. 3.

<sup>d</sup>Confidence intervals of model predictions (95%).

<sup>e</sup> $T_{\text{max}}$ , maximal temperature for growth.

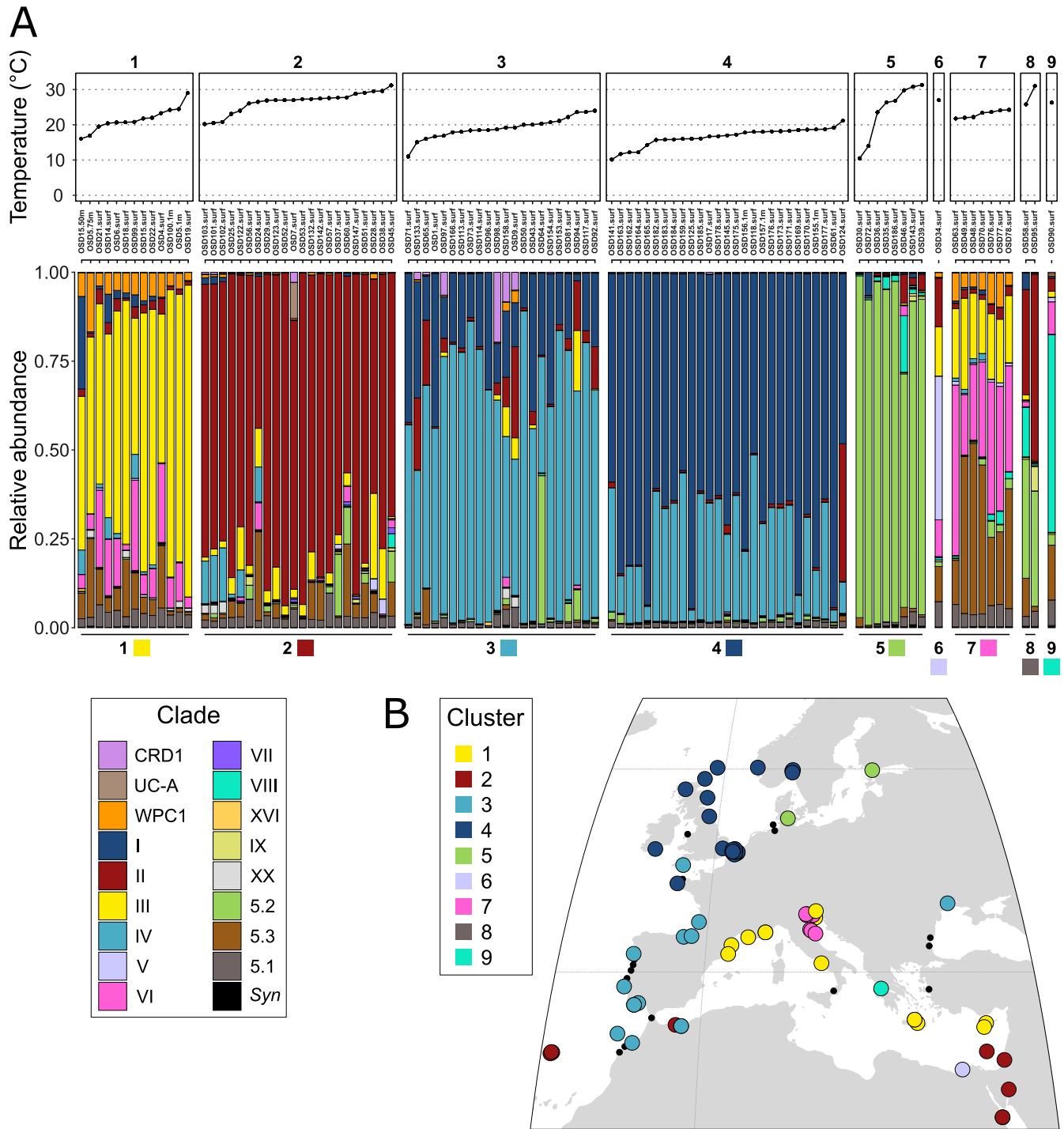


**FIG 3** Clusters of Ocean Sampling Day (OSD) stations based on relative abundance profiles of *Synechococcus* clades. OSD stations were clustered based on the relative abundance profiles of marine *Synechococcus* clades using Bray-Curtis distance: two stations will cluster together if they have a similar composition in *Synechococcus* clades. The clustering dendrogram is available as Fig. S2. (A) The upper panel indicates water temperature. The lower panel shows the nine clusters of relative abundance profiles of *Synechococcus* clades. Categories 5.1 and *Syn* correspond to reads that could not be assigned to a clade but were assigned to the higher taxonomic levels of *Synechococcus* SC 5.1 or *Synechococcus* genus, respectively. (B) Geographical distribution of the nine clusters of OSD stations along the European coasts. A global map of cluster distribution is available as Fig. S3.

IV strain isolated in the Mediterranean Sea (40). Thus, the ecological drivers of clades I and IV distribution may be difficult to identify due to underlying differences within each clade, and a finer taxonomic resolution might be necessary to observe a significant effect of temperature on the distribution of these populations.

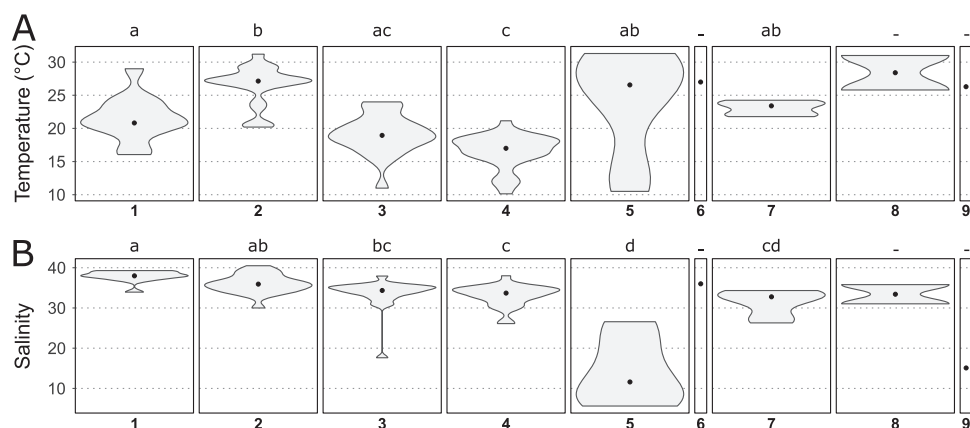


**FIG 4** Violin plots showing the distribution of temperature and salinity for each cluster of Ocean Sampling Day (OSD) stations defined in Fig. 3. (A) Temperature. (B) Salinity. Panels are numbered according to cluster numbers in Fig. 3. The black dot in each violin plot shows the median value. Different letters indicate significantly different distributions (Dunn test, adjusted  $P$ -value < 0.05). The same analysis considering distance to the nearest coast gave no significant result.

**Local changes in *Synechococcus* communities in the Mediterranean Sea.** Stations sampled in the Mediterranean Sea fell into several clusters based on their composition in *Synechococcus*/*Cyanobium* lineages. Most stations belonged to cluster 1, dominated by clade III with a low relative abundance of clades VI, WPC1 and SC 5.3 (Fig. 3). This composition is quite similar to that previously described by Farrant et al. (12) for open waters of the Mediterranean Sea, which was suggested to be related to specific features of this semi-enclosed sea and notably to its low phosphate concentration (12, 15, 30). Most of the stations of the Adriatic Sea formed a distinct cluster (cluster 7), where the same clades were present but in different proportions, clade VI and SC 5.3 taking over clade III. Finally, stations OSD34 and OSD90, located on the Egyptian and Greek coasts, respectively, the only stations of the OSD data set comprising a high proportion of clade V or VIII, formed a cluster on their own (clusters 6 and 9, respectively). While these 4 clusters (clusters 1, 6, 7, and 9) are specific to the Mediterranean Sea, it is worth noting that 2 stations at the easternmost end of the Mediterranean Sea (OSD123 and OSD132) (Fig. 3 and Fig. S1) fell into cluster 2, dominated by clade II, and showed a clade composition very similar to the samples collected in the Red Sea (OSD52 and OSD53). While this observation could be due to similar environmental conditions in the Eastern Mediterranean Sea and the Red Sea, it also suggests that Israeli coastal areas may be influenced by waters entering the Mediterranean Sea via the Suez Canal, consistent with previous findings for *Synechococcus*, *Prochlorococcus*, as well as for many larger organisms (63, 64). Indeed, the water has been estimated to flow northward through the Canal until the end of June with up to  $1250 \text{ m}^3 \text{ s}^{-1}$ , facilitating species migrations to the Mediterranean Sea (65).

Interestingly, the 3 specific clusters identified in the Mediterranean Sea displayed different temperature and salinity characteristics (Fig. 4A and B). The salinity range of stations in cluster 1 (dominated by clade III) was narrow (average salinity 37.90 psu, median 37.98 psu) and significantly higher than that of cluster 7 (dominated by clade VI and SC 5.3, average salinity 31.43 psu, median 32.77 psu), suggesting that clade VI and SC 5.3 are able to cope with lower salinities. Consistently, SC 5.3 was recently found to encompass members colonizing freshwater lakes (25, 33), while in the marine environment, this subcluster was reported both in strictly marine waters (12, 31) and in low salinity waters (66). Our study also brings new insights into the ecological niche occupied by clade VI, whose distribution was so far poorly known (30), and that appears to be restricted to coastal regions of intermediate salinity. All stations of the Adriatic Sea comprising cluster 6 were indeed sampled in the northwestern part of this area, where the influence of the Po River plume may be important (67). This distribution is consistent with previous observations of the closely related, and often co-occurring, clade V in low salinity surface



waters of the Adriatic Sea (49) and of both clades V and VI in the Pearl River Estuary (23). Laboratory experiments also showed that representative strains of these 2 clades can tolerate salinities as low as 15 psu (68). Still, we cannot exclude that besides low salinity, other local specificities linked to riverine input might also explain the predominance of SC 5.3 and clade VI in coastal areas of the Adriatic Sea.

A significant difference in water temperature was also found between cluster 1, dominated by clade III (average temperature 21.5°C, median 20.8°C) and cluster 2, dominated by clade II (average 26.5°C, median 27.1°C). This suggests that the shift observed at the easternmost part of the Mediterranean Sea from a dominance of clade III to a local dominance of clade II (stations OSD123 and OSD132) (Fig. 1 and Fig. S1) might be related to a difference in water temperature. Interestingly, in contrast to clades I and IV that often co-occur, clades II and III seem to be nearly mutually exclusive, at least in the Mediterranean Sea, and the temperature limit above which clade II dominates seems to lie around 25°C (Fig. 3). In our experimental comparison of thermal preferences, this corresponds to the temperature at which growth rates of clade II strains become higher than that of clade III strains, resulting in a higher optimal temperature of clade II compared to clade III strains (Table 2). Altogether, temperature and salinity appear as major factors driving the composition of *Synechococcus/Cyanobium* communities in coastal waters of the Mediterranean Sea, although other biotic and abiotic factors are most likely involved, notably the availability of phosphorus, a key limiting nutrient in this area (69).

**Conclusion.** The OSD data set is unique, not only by providing an instantaneous snapshot of the microbial community composition but also because, by focusing on coastal areas, it nicely complements other recent global ocean surveys performed in the open ocean (5, 12, 32, 37, 70, 71). In particular, the good spatial resolution of the sampling performed along the European coasts is well-adapted to observe shifts in communities and delineate their boundaries. Despite the fact that only a few physico-chemical parameters were collected, this data set allowed us to considerably improve our knowledge of the distribution of *Synechococcus/Cyanobium* lineages in coastal areas, to gain insights into the realized environmental niches of the main ones, including some that were previously poorly known such as clade VI, as well as to reinforce hypotheses about thermal niche differentiation that were supported by laboratory experiments on a set of representative strains. Still, it is likely that the shifts observed here at the summer solstice would exhibit different latitudinal boundaries at other seasons since time series studies of *Synechococcus* community composition have revealed strong seasonal patterns, notably due the succession of different thermotypes (48, 50, 58, 60, 62). A continued effort toward global instantaneous surveys of microbial diversity in coastal areas over the long term and at different seasons would be invaluable to monitor the evolution of microbial communities in relation to global change.

## MATERIALS AND METHODS

**OSD metagenomics data.** OSD 2014 is a global sampling campaign that took place on June 21<sup>st</sup>, 2014 and sampled 157 stations worldwide for metagenomes (Table S1). The median distance to the nearest coast was 0.29 nautical miles (average: 6.3 nautical miles). Details about sampling methods can be found in (72) and at <https://github.com/ocean-sampling-day/OSD2014>. Data were downloaded from the EBI (see data availability below) for 150 of the 157 stations for which a “processed reads without annotation” file was available, generated following the EBI analysis pipeline v2.0, available at <https://www.ebi.ac.uk/metagenomics/pipelines/2.0>. Briefly, Illumina MiSeq paired reads were merged using SeqPrep (<https://github.com/jstjohn/seqprep>) and trimmed for low quality ends, then sequences with more than 10% undetermined nucleotides were removed using Trimmomatic (73) before discarding reads shorter than 100 nucleotides. Contextual data were downloaded from PANGEA (<https://doi.pangaea.de/10.1594/PANGAEA.854419>) and the data used in this study are listed in Table S1: as the contextual data are very sparse for most parameters, we only used water temperature and salinity data that were available for a sufficient number of stations. A map of OSD stations used in this study is available as Fig. S1.

**Taxonomic assignment of metagenomic reads.** Because OSD metagenomes were not sequenced deeply enough to rely on a single high resolution marker gene for taxonomic assignment (12, 74), we used a Whole Genome Recruitment (WGR; [75, 76]) approach against a reference genome database of 863 publicly available complete genomes of aquatic bacteria (Table S2). The latter encompassed 141

genomes of marine picocyanobacteria as well as 722 cyanobacterial or other aquatic microbial genomes, including 185 cyanobacterial genomes other than *Prochlorococcus* and marine *Synechococcus* listed in Cyanobase, (<http://genome.microbedb.jp/cyanobase/>) as well as 537 genomes of other aquatic microbes downloaded from the proGenomes database (<http://progenomes.embl.de/representatives.cgi>). This large number of outgroup genomes representative of the known diversity of the oceans was selected to minimize the risk of unspecific mapping on picocyanobacterial genomes.

BLASTN (v2.2.28+) (77, 78) was used to align metagenomic reads against this reference database. Only best-hit matches (option `-max_target_seqs 1`) with an e-value below  $10^{-3}$  (e-value 0.001) were kept, and reads matching outgroup genomes were discarded. Based on BLASTN results, reads aligning over more than 90% of their length on a picocyanobacterial genome were extracted from initial read files, and a second BLASTN was run against a database containing only marine picocyanobacterial genomes with default parameters except for a lower limit on percentage of identity of 30% (`-perc_identity 30`), a filter on e-value of  $10^{-2}$  (e-value 0.01), and by selecting the blastn algorithm (`-task blastn`) to allow for reads to map on multiple reference genomes. BLASTN results were then parsed using the Lowest Common Ancestor method (79). For each read, BLAST matches with over 80% identity, corresponding to a major discontinuity of the average nucleotide identity (ANI) values within the marine picocyanobacteria radiation (20), aligned over more than 90% of their length against a reference genome were kept if their BLAST score was within 5% of the best score. Then, the read was attributed to the lowest common ancestor of these matches (i.e., strain, clade, subcluster, or genus). Counts of reads assigned to the strain or subclade levels were ultimately aggregated by clade. Two additional categories were made for reads that could only be assigned to the level of *Synechococcus* subcluster 5.1 (SC 5.1 in Fig. 1 and 3) or even *Synechococcus* genus (*Syn* in Fig. 1 and 3). With such a method, potential remaining unspecifically mapped reads that would not have been filtered out by our first filter are highly unlikely to be assigned to the clade level. Moreover, this method allows to be very conservative on the taxonomic assignment of reads, and to avoid any misannotation of reads mapping to conserved regions of the genome.

**Analysis of picocyanobacterial community composition.** In order to account for the potential variation in genome length among clades, read counts were divided by the average genome length within each clade. To minimize the noise in recruitment data, we then removed from the data set stations with less than 600 recruited reads per million bp, corresponding to a genome coverage of ca. 16%, since reads are 242 bp long on average. Read counts at each station were further normalized by the total number of picocyanobacterial reads recruited at this station to assess relative abundances of taxa with the function `decostand` in R package `vegan` v2.2-1 (80). Bray-Curtis distances based on relative abundances were computed with function `vegdist` (`method="Bray"`) in R package `vegan` v2.2-1 (80), and used to cluster stations with function `agnes` in R package `cluster` v1.14.4 (81) with the default method "average" (unweighted pair-group arithmetic average method, UPGMA). The resulting clustering dendrogram and the cutoff used to delineate clusters are represented on Fig. S2. Figures were drawn in R v3.0.3 with package `ggplot2` v1.0.1 (82).

**Thermal preferences of strains representative of the most abundant clades *in situ*.** Two strains of each of the 4 most abundant *Synechococcus* clades in Fe-replete areas (clades I to IV) were selected from the Roscoff Culture Collection (Table 1) (<http://roscoff-culture-collection.org/>; [83]). Strains were grown in polystyrene flasks in PCR-S11 medium (84) supplemented with 1 mM sodium nitrate. The seawater was reconstituted using Red Sea Salts and distilled water. Cultures of the 8 strains were acclimated at least 2 weeks to a range of temperatures from 10°C to 33°C, within temperature-controlled chambers (Liebherr-Hausgeräte) and continuous light was provided by green/white/blue LEDs (Alpheus) at an irradiance of  $20 \mu\text{mol photons m}^{-2} \text{s}^{-1}$ . After acclimation, cultures were split into 3 biological replicates for each strain, and sampled once or twice a day until the stationary phase was reached.

For cell density measurements, aliquots of cultures were preserved with 0.25% glutaraldehyde grade II (Sigma-Aldrich) and stored at  $-80^\circ\text{C}$  until analysis (85). Cell concentration was determined using a flow cytometer (FACSCanto II, Becton, Dickinson) with laser emission set at 488 nm, and using distilled water as sheath fluid.

To estimate the maximum population growth rates, we used the following equation:

$$\frac{dN}{dt} = \mu N$$

Where  $N$  is the cell abundances (in cells  $\text{mL}^{-1}$ ) and  $\mu$  is the maximum population growth rate (in  $\text{days}^{-1}$ ). We estimated  $\mu$  as the coefficient of the linear regression model performed on log-transform  $N(t)$  data during the exponential phase only.

To overcome the fact that discrete experimental measurements have a limited resolution, we estimated the cardinal growth parameters for each strain using the Cardinal Temperature Model with Inflection (BR model; 86), which describes the maximal phytoplankton growth rate ( $\mu_{\text{max}}$ ) as a function of temperature ( $T$ ) as follows:

$$\mu_{\text{max}} = \begin{cases} 0 & \text{for } T < T_{\text{min}} \\ \mu_{\text{opt}} \phi(T) & \text{for } T_{\text{min}} < T < T_{\text{max}} \\ 0 & \text{for } T > T_{\text{max}} \end{cases} \quad (1)$$

where:

$$\phi(T) = \frac{(T - T_{\max})(T - T_{\min})^2}{(T_{\text{opt}} - T_{\min})[(T_{\text{opt}} - T_{\min})(T - T_{\text{opt}}) - (T_{\text{opt}} - T_{\max})(T_{\text{opt}} + T_{\min} - 2T)]} \quad (2)$$

$T_{\min}$  and  $T_{\max}$  are the minimal and maximal growth temperatures and  $T_{\text{opt}}$  is the optimal growth temperature where  $\mu_{\max} = \mu_{\text{opt}}$ . We estimated the cardinal growth temperatures ( $T_{\min}$ ,  $T_{\text{opt}}$ ,  $T_{\max}$ ) and the optimal growth rate ( $\mu_{\text{opt}}$ ) using the same procedure as in (86). Briefly, we used *Synechococcus* experimental growth rates obtained at different temperatures and fitted equations 1 and 2 by minimizing the Euclidian distance (fitting error) between model and data (Residual Sum of Squares) using the Scilab *leastsq* function. More information on the fitting procedure can be found in ([86]; section 2.2, parameter identification). Because of the shape of the growth response curve and the variability in the experimental data for low temperatures, our data did not allow to constrain  $T_{\min}$ , but this did not affect our estimation of other parameters (Table 2).

**Data availability.** Metagenomic data are available from the European Nucleotide Archive (<http://www.ebi.ac.uk/ena/data/view/PRJEB8682>) under the study accession number PRJEB8682 (raw data) and from the European Bioinformatics Institute (EBI) Metagenomics portal under the project accession number ERP009703 (processed data). Contextual data collected at all OSD stations were retrieved from PANGAEA (<https://doi.pangaea.de/10.1594/PANGAEA.854419>; Ocean Sampling Day Consortium, 2015). All genomes of aquatic bacteria used as reference or outgroups in this study are publicly available and their database origin and accession numbers are listed in Table S2.

## SUPPLEMENTAL MATERIAL

Supplemental material is available online only.

**FIG S1**, PDF file, 2.3 MB.

**FIG S2**, PDF file, 0.4 MB.

**FIG S3**, PDF file, 0.8 MB.

**TABLE S1**, XLSX file, 0.03 MB.

**TABLE S2**, XLSX file, 0.1 MB.

## ACKNOWLEDGMENTS

We thank the OSD Consortium for sampling, sequencing, and making the data analyzed in this paper available, as well as the Roscoff Culture Collection (<http://roscoff-culture-collection.org/>) for providing *Synechococcus* strains used in this study.

Financial support for the OSD program was provided by the European Union program MicroB3 (UE-contract-287589) and authors were supported by the French “Agence Nationale de la Recherche” programs SAMOSA (ANR-13-ADAP-0010) and CINNAMON (ANR-17-CE02-0014-01), as well as the European program Assemble Plus (H2020-INFRAIA-1-2016-2017; grant no. 730984).

D.J.S. received funding from the European Research Council (ERC) under the European Union’s Horizon 2020 research and innovation program (grant agreement No 883551).

We declare no competing interests.

## REFERENCES

- Flombaum P, Gallegos JL, Gordillo RA, Rincón J, Zabala LL, Jiao N, Karl DM, Li WKW, Lomas MW, Veneziano D, Vera CS, Vrugt JA, Martiny AC. 2013. Present and future global distributions of the marine Cyanobacteria *Prochlorococcus* and *Synechococcus*. *Proc Natl Acad Sci U S A* 110: 9824–9829. <https://doi.org/10.1073/pnas.1307701110>.
- Partensky F, Blanchot J, Vaulot D. 1999. Differential distribution and ecology of *Prochlorococcus* and *Synechococcus* in oceanic waters: a review. *Bull L’institut Océanographique* 19:457–475. <https://www.documentation.ird.fr/hor/fdi:010019783>.
- Johnson ZI, Zinser ER, Coe A, McNulty NP, Woodward EMS, Chisholm SW. 2006. Niche partitioning among *Prochlorococcus* ecotypes along ocean-scale environmental gradients. *Science* 311:1737–1740. <https://doi.org/10.1126/science.1118052>.
- Paulsen ML, Doré H, Garczarek L, Seuthe L, Müller O, Sandaa R-A, Bratbak G, Larsen A. 2016. *Synechococcus* in the Atlantic Gateway to the Arctic Ocean. *Front Mar Sci* 3. <https://doi.org/10.3389/fmars.2016.00191>.
- Kent AG, Baer SE, Mouginito C, Huang JS, Larkin AA, Lomas MW, Martiny AC. 2019. Parallel phylogeography of *Prochlorococcus* and *Synechococcus*. *ISME J* 13:430–441. <https://doi.org/10.1038/s41396-018-0287-6>.
- Xia X, Cheung S, Endo H, Suzuki K, Liu H. 2019. Latitudinal and vertical variation of *Synechococcus* assemblage composition along 170° W transect from the South Pacific to the Arctic Ocean. *Microb Ecol* 77:333–342. <https://doi.org/10.1007/s00248-018-1308-8>.
- Visintini N, Martiny AC, Flombaum P. 2021. *Prochlorococcus*, *Synechococcus*, and picoeukaryotic phytoplankton abundances in the global ocean. *Limnol Oceanogr Lett* 6:207–215. <https://doi.org/10.1002/lol2.10188>.
- Scanlan DJ. 2012. Marine picocyanobacteria, p 503–533. *In* Whitton BA (ed), *Ecology of cyanobacteria II: their diversity in space and time*. Springer, Dordrecht, Netherlands.
- Dufresne A, Ostrowski M, Scanlan DJ, Garczarek L, Mazard S, Palenik BP, Paulsen IT, de Marsac NT, Wincker P, Dossat C, Ferriera S, Johnson J, Post AF, Hess WR, Partensky F. 2008. Unraveling the genomic mosaic of a ubiquitous genus of marine cyanobacteria. *Genome Biol* 9:R90. <https://doi.org/10.1186/gb-2008-9-5-r90>.
- Mazard S, Ostrowski M, Partensky F, Scanlan DJ. 2012. Multi-locus sequence analysis, taxonomic resolution and biogeography of marine *Synechococcus*. *Environ Microbiol* 14:372–386. <https://doi.org/10.1111/j.1462-2920.2011.02514.x>.
- Rocap G, Larimer FW, Lamerdin J, Malfatti S, Chain P, Ahlgren NA, Arellano A, Coleman M, Hauser L, Hess WR, Johnson ZI, Land M, Lindell D, Post AF, Regala W, Shah M, Shaw SL, Steglich C, Sullivan MB, Ting CS, Tolonen A, Webb EA, Zinser ER, Chisholm SW. 2003. Genome divergence

- in two *Prochlorococcus* ecotypes reflects oceanic niche differentiation. *Nature* 424:1042–1047. <https://doi.org/10.1038/nature01947>.
12. Farrant GK, Doré H, Cornejo-Castillo FM, Partensky F, Ratin M, Ostrowski M, Pitt FD, Wincker P, Scanlan DJ, Iudicone D, Acinas SG, Garczarek L. 2016. Delineating ecologically significant taxonomic units from global patterns of marine picocyanobacteria. *Proc Natl Acad Sci U S A* 113: E3365–E3374.
  13. Garcia CA, Hagstrom GI, Larkin AA, Ustick LJ, Levin SA, Lomas MW, Martiny AC. 2020. Linking regional shifts in microbial genome adaptation with surface ocean biogeochemistry. *Philos Trans R Soc Lond B Biol Sci*: 375. <https://doi.org/10.1098/rstb.2019.0254>.
  14. Moore LR, Rocap G, Chisholm SW. 1998. Physiology and molecular phylogeny of coexisting *Prochlorococcus* ecotypes. *Nature* 393:464–467. <https://doi.org/10.1038/30965>.
  15. Mella-Flores D, Mazard S, Humily F, Partensky F, Mahé F, Bariati L, Courties C, Marie D, Ras J, Mauriac R, Jeanthon C, Mahdi Bendif E, Ostrowski M, Scanlan DJ, Garczarek L. 2011. Is the distribution of *Prochlorococcus* and *Synechococcus* ecotypes in the Mediterranean Sea affected by global warming? *Biogeosciences* 8:2785–2804. <https://doi.org/10.5194/bg-8-2785-2011>.
  16. Chandler JW, Lin Y, Gainer PJ, Post AF, Johnson ZI, Zinser ER. 2016. Variable but persistent coexistence of *Prochlorococcus* ecotypes along temperature gradients in the ocean's surface mixed layer. *Environ Microbiol Rep* 8:272–284. <https://doi.org/10.1111/1758-2229.12378>.
  17. Malmstrom RR, Rodrigue S, Huang KH, Kelly L, Kern SE, Thompson A, Roggensack S, Berube PM, Henn MR, Chisholm SW. 2013. Ecology of uncultured *Prochlorococcus* clades revealed through single-cell genomics and biogeographic analysis. *ISME J* 7:184–198. <https://doi.org/10.1038/ismej.2012.89>.
  18. Rusch DB, Martiny AC, Dupont CL, Halpern AL, Venter JC. 2010. Characterization of *Prochlorococcus* clades from iron-depleted oceanic regions. *Proc Natl Acad Sci U S A* 107:16184–16189. <https://doi.org/10.1073/pnas.1009513107>.
  19. Herdman M, Castenholz RW, Waterbury JB, Rippka R. 2001. Form-genus XIII. *Synechococcus*, p 508–512. In Boone D, Castenholz R (ed), *Bergey's manual of systematics of Archaea and Bacteria* volume 12nd edition. Springer-Verlag, New York, NY.
  20. Doré H, Farrant GK, Guyet U, Haguait J, Humily F, Ratin M, Pitt FD, Ostrowski M, Six C, Brillet-Guéguen L, Hoebeke M, Bisch A, Le Corguillé G, Corre E, Labadie K, Aury JM, Wincker P, Choi DH, Noh JH, Eveillard D, Scanlan DJ, Partensky F, Garczarek L. 2020. Evolutionary mechanisms of long-term genome diversification associated with niche partitioning in marine picocyanobacteria. *Front Microbiol* 11. <https://doi.org/10.3389/fmicb.2020.567431>.
  21. Chen F, Wang K, Kan J, Suzuki MT, Wommack KE. 2006. Diverse and unique picocyanobacteria in Chesapeake Bay, revealed by 16S-23S rRNA internal transcribed spacer sequences. *Appl Environ Microbiol* 72:2239–2243. <https://doi.org/10.1128/AEM.72.3.2239-2243.2006>.
  22. Cai H, Wang K, Huang S, Jiao N, Chen F. 2010. Distinct patterns of picocyanobacterial communities in winter and summer in the Chesapeake Bay. *Appl Environ Microbiol* 76:2955–2960. <https://doi.org/10.1128/AEM.02868-09>.
  23. Xia X, Guo W, Tan S, Liu H. 2017. *Synechococcus* assemblages across the salinity gradient in a salt wedge estuary. *Front Microbiol* 8:1254. <https://doi.org/10.3389/fmicb.2017.01254>.
  24. Hunter-Cevera KR, Post AF, Peacock EE, Sosik HM. 2016. Diversity of *Synechococcus* at the Martha's Vineyard Coastal Observatory: insights from culture isolations, clone libraries, and flow cytometry. *Microb Ecol* 71: 276–289. <https://doi.org/10.1007/s00248-015-0644-1>.
  25. Cabello-Yeves PJ, Picazo A, Camacho A, Callieri C, Rosselli R, Roda-Garcia JJ, Coutinho FH, Rodriguez-Valera F. 2018. Ecological and genomic features of two widespread freshwater picocyanobacteria. *Environ Microbiol* 20:3757–3771. <https://doi.org/10.1111/1462-2920.14377>.
  26. Chen F, Wang K, Kan J, Bachoon DS, Lu J, Lau S, Campbell L. 2004. Phylogenetic diversity of *Synechococcus* in the Chesapeake Bay revealed by Ribulose-1,5-bisphosphate carboxylase-oxygenase (RuBisCO) large subunit gene (*rbcL*) sequences. *Aquat Microb Ecol* 36:153–164. <https://doi.org/10.3354/ame036153>.
  27. Xia X, Partensky F, Garczarek L, Suzuki K, Guo C, Cheung SY, Liu H. 2017. Phylogeography and pigment type diversity of *Synechococcus* cyanobacteria in surface waters of the northwestern Pacific Ocean. *Environ Microbiol* 19:142–158. <https://doi.org/10.1111/1462-2920.13541>.
  28. Xia X, Vidyarthana NK, Palenik B, Lee P, Liu H. 2015. Comparison of the seasonal variations of *Synechococcus* assemblage structures in estuarine waters and coastal waters of Hong Kong. *Appl Environ Microbiol* 81: 7644–7655. <https://doi.org/10.1128/AEM.01895-15>.
  29. Haverkamp T, Acinas SG, Doeleman M, Stomp M, Huisman J, Stal LJ. 2008. Diversity and phylogeny of Baltic Sea picocyanobacteria inferred from their ITS and phycobiliprotein operons. *Environ Microbiol* 10:174–188. <https://doi.org/10.1111/j.1462-2920.2007.01442.x>.
  30. Zwirgmaier K, Jardillier L, Ostrowski M, Mazard S, Garczarek L, Vault D, Not F, Massana R, Ulloa O, Scanlan DJ. 2008. Global phylogeography of marine *Synechococcus* and *Prochlorococcus* reveals a distinct partitioning of lineages among oceanic biomes. *Environ Microbiol* 10:147–161. <https://doi.org/10.1111/j.1462-2920.2007.01440.x>.
  31. Huang S, Wilhelm SW, Harvey HR, Taylor K, Jiao N, Chen F. 2012. Novel lineages of *Prochlorococcus* and *Synechococcus* in the global oceans. *ISME J* 6:285–297. <https://doi.org/10.1038/ismej.2011.106>.
  32. Sohm JA, Ahlgren NA, Thomson ZJ, Williams C, Moffett JW, Saito MA, Webb EA, Rocap G. 2015. Co-occurring *Synechococcus* ecotypes occupy four major oceanic regimes defined by temperature, macronutrients and iron. *ISME J* 10:333–345. <https://doi.org/10.1038/ismej.2015.115>.
  33. Cabello-Yeves PJ, Haro-Moreno JM, Martin-Cuadrado AB, Ghai R, Picazo A, Camacho A, Rodriguez-Valera F. 2017. Novel *Synechococcus* genomes reconstructed from freshwater reservoirs. *Front Microbiol* 8:1–13. <https://doi.org/10.3389/fmicb.2017.01151>.
  34. Urbach E, Robertson DL, Chisholm SW. 1992. Multiple evolutionary origins of prochlorophytes within the cyanobacterial radiation. *Nature* 355: 267–270. <https://doi.org/10.1038/355267a0>.
  35. Sánchez-Baracaldo P. 2015. Origin of marine planktonic cyanobacteria. *Sci Rep* 5:17418. <https://doi.org/10.1038/srep17418>.
  36. Fuller NJ, Marie D, Partensky F, Vault D, Post AF, Scanlan DJ. 2003. Clade-specific 16S ribosomal DNA oligonucleotides reveal the predominance of a single marine *Synechococcus* clade throughout a stratified water column in the Red Sea. *Appl Environ Microbiol* 69:2430–2443. <https://doi.org/10.1128/AEM.69.5.2430-2443.2003>.
  37. Ahlgren NA, Belisle BS, Lee MD. 2020. Genomic mosaicism underlies the adaptation of marine *Synechococcus* ecotypes to distinct oceanic iron niches. *Environ Microbiol* 22:1801–1815. <https://doi.org/10.1111/1462-2920.14893>.
  38. Ferrieux M, Dufour L, Doré H, Ratin M, Guéneuguès A, Chasselin L, Marie D, Rigaut-Jalabert F, Le Gall F, Sciandra T, Monier G, Hoebeke M, Corre E, Xia X, Liu H, Scanlan DJ, Partensky F, Garczarek L. 2022. Comparative thermophysiology of marine *Synechococcus* CRD1 strains isolated from different thermal niches in iron-depleted areas. *Front Microbiol* 13. <https://doi.org/10.3389/fmicb.2022.893413>.
  39. Pittera J, Humily F, Thorel M, Grulois D, Garczarek L, Six C. 2014. Connecting thermal physiology and latitudinal niche partitioning in marine *Synechococcus*. *ISME J* 8:1221–1236. <https://doi.org/10.1038/ismej.2013.228>.
  40. Breton S, Jouhet J, Guyet U, Gros V, Pittera J, Demory D, Partensky F, Doré H, Ratin M, Maréchal E, Nguyen NA, Garczarek L, Six C. 2020. Unveiling membrane thermoregulation strategies in marine picocyanobacteria. *New Phytol* 225:2396–2410. <https://doi.org/10.1111/nph.16239>.
  41. Mackey KRM, Paytan A, Caldeira K, Grossman AR, Moran D, McIlvin M, Saito MA. 2013. Effect of temperature on photosynthesis and growth in marine *Synechococcus* spp. *Plant Physiol* 163:815–829. <https://doi.org/10.1104/pp.113.221937>.
  42. Varkey D, Mazard S, Ostrowski M, Tetu SG, Haynes P, Paulsen IT. 2016. Effects of low temperature on tropical and temperate isolates of marine *Synechococcus*. *ISME J* 10:1252–1263. <https://doi.org/10.1038/ismej.2015.179>.
  43. Pittera J, Partensky F, Six C. 2017. Adaptive thermostability of light-harvesting complexes in marine picocyanobacteria. *ISME J* 11:112–124. <https://doi.org/10.1038/ismej.2016.102>.
  44. Pittera J, Jouhet J, Breton S, Garczarek L, Partensky F, Maréchal É, Nguyen NA, Doré H, Ratin M, Pitt FD, Scanlan DJ, Six C. 2018. Thermoacclimation and genome adaptation of the membrane lipidome in marine *Synechococcus*. *Environ Microbiol* 20:612–631. <https://doi.org/10.1111/1462-2920.13985>.
  45. Xia X, Liu H, Choi D, Noh JH. 2018. Variation of *Synechococcus* pigment genetic diversity along two turbidity gradients in the China Seas. *Microb Ecol* 75:10–21. <https://doi.org/10.1007/s00248-017-1021-z>.
  46. Tai V, Palenik B. 2009. Temporal variation of *Synechococcus* clades at a coastal Pacific Ocean monitoring site. *ISME J* 3:903–915. <https://doi.org/10.1038/ismej.2009.35>.
  47. Hunter-Cevera KR, Neubert MG, Solow AR, Olson RJ, Shalapyonok A, Sosik HM. 2014. Diel size distributions reveal seasonal growth dynamics of a coastal phytoplankton. *Proc Natl Acad Sci U S A* 111:9852–9857. <https://doi.org/10.1073/pnas.1321421111>.

48. Nagarkar M, Wang M, Valencia B, Palenik B. 2021. Spatial and temporal variations in *Synechococcus* microdiversity in the Southern California coastal ecosystem. *Environ Microbiol* 23:252–266. <https://doi.org/10.1111/1462-2920.15307>.
49. Šilović T, Balagué V, Orlić S, Pedrós-Alió C. 2012. Picoplankton seasonal variation and community structure in the northeast Adriatic coastal zone. *FEMS Microbiol Ecol* 82:678–691. <https://doi.org/10.1111/j.1574-6941.2012.01438.x>.
50. Larkin AA, Moreno AR, Fagan AJ, Fowlds A, Ruiz A, Martiny AC. 2020. Persistent El Niño driven shifts in marine cyanobacteria populations. *PLoS One* 15:e0238405. <https://doi.org/10.1371/journal.pone.0238405>.
51. Kopf A, Bicak M, Kottmann R, Schnetzer J, Kostadinov I, Lehmann K, Fernandez-Guerra A, Jeanthon C, Rahav E, Ullrich M, Wichels A, Gerdtts G, Polymenakou P, Kotoulas G, Siam R, Abdallah RZ, Sonnenschein EC, Cariou T, O'Gara F, Jackson S, Orlic S, Steinke M, Busch J, Duarte B, Caçador A, Canning-Clode J, Bobrova O, Marteinsson V, Reynisson E, Loureiro CM, Luna GM, Quero GM, Löscher CR, Kremp A, DeLorenzo ME, Øvreås L, Tolman J, LaRoche J, Penna A, Frischer M, Davis T, Katherine B, Meyer CP, Ramos S, Magalhães C, Jude-Lemelleur F, Aguirre-Macedo ML, Wang S, Poulton N, Jones S, et al. 2015. The ocean sampling data consortium. *Gigascience* 4:27. <https://doi.org/10.1186/s13742-015-0066-5>.
52. Olson RJ, Chisholm SW, Zettler ER, Altabet MA, Dusenberry JA. 1990. Spatial and temporal distributions of prochlorophyte picoplankton in the North Atlantic Ocean. *Deep Sea Res A, Oceanogr Res Pap* 37:1033–1051. [https://doi.org/10.1016/0198-0149\(90\)90109-9](https://doi.org/10.1016/0198-0149(90)90109-9).
53. Six C, Ratin M, Marie D, Corre E. 2021. Marine *Synechococcus* picocyanobacteria: light utilization across latitudes. *Proc Natl Acad Sci U S A* 118:e2111300118. <https://doi.org/10.1073/pnas.2111300118>.
54. Moore LR, Goericke R, Chisholm SW. 1995. Comparative physiology of *Synechococcus* and *Prochlorococcus*: influence of light and temperature on growth, pigments, fluorescence and absorptive properties. *Mar Ecol Prog Ser* 116:259–275. <https://doi.org/10.3354/meps116259>.
55. Scanlan DJ, Ostrowski M, Mazard S, Dufresne A, Garczarek L, Hess WR, Post AF, Hagemann M, Paulsen I, Partensky F. 2009. Ecological genomics of marine picocyanobacteria. *Microbiol Mol Biol Rev* 73:249–299. <https://doi.org/10.1128/MMBR.00035-08>.
56. Babic I, Petric I, Bosak S, Mihanovic H, Dupcic Radic I, Ljubecic Z. 2017. Marine Genomics distribution and diversity of marine picocyanobacteria community: targeting of *Prochlorococcus* ecotypes in winter conditions (Southern Adriatic Sea). *Mar Genomics* 36: 3–11. <https://doi.org/10.1016/j.margen.2017.05.014>.
57. Choi DH, Noh JH, An SM, Choi YR, Lee H, Ra K, Kim D, Rho T, Lee SH, Kim KT, Chang KI, Lee JH. 2016. Spatial distribution of cold-adapted *Synechococcus* during spring in seas adjacent to Korea. *Algae* 31:231–241. <https://doi.org/10.4490/algae.2016.31.9.10>.
58. Choi DH, Noh JH, Shim J. 2013. Seasonal changes in picocyanobacterial diversity as revealed by pyrosequencing in temperate waters of the East China Sea and the East Sea. *Aquat Microb Ecol* 71:75–90. <https://doi.org/10.3354/ame01669>.
59. Tai V, Burton R, Palenik B. 2011. Temporal and spatial distributions of marine *Synechococcus* in the Southern California Bight assessed by hybridization to bead-arrays. *Mar Ecol Prog Ser* 426:133–147. <https://doi.org/10.3354/meps09030>.
60. Hunter-Cevera KR, Hamilton BR, Neubert MG, Sosik HM. 2021. Seasonal environmental variability drives microdiversity within a coastal *Synechococcus* population. *Environ Microbiol* 23:4689–4705. <https://doi.org/10.1111/1462-2920.15666>.
61. Ahlgren NA, Perelman JN, Yeh Y-C, Fuhrman JA. 2019. Multi-year dynamics of fine-scale marine cyanobacterial populations are more strongly explained by phage interactions than abiotic, bottom-up factors. *Environ Microbiol* 21:2948–2963. <https://doi.org/10.1111/1462-2920.14687>.
62. Mackey KRM, Hunter-Cevera K, Britten GL, Murphy LG, Sogin ML, Huber JA. 2017. Seasonal succession and spatial patterns of *Synechococcus* microdiversity in a salt marsh estuary revealed through 16S rRNA gene oligotyping. *Front Microbiol* 8:1–11. <https://doi.org/10.3389/fmicb.2017.01496>.
63. Feingersch R, Suzuki MT, Shmoish M, Sharon I, Sabehi G, Partensky F, Beja O. 2010. Microbial community genomics in eastern Mediterranean Sea surface waters. *ISME J* 4:78–87. <https://doi.org/10.1038/ismej.2009.92>.
64. Katsanevakis S, Coll M, Piroddi C, Steenbeek J, Ben Rais Lasram F, Zenetos A, Cardoso AC. 2014. Invading the Mediterranean Sea: biodiversity patterns shaped by human activities. *Front Mar Sci* 1:1–11. <https://doi.org/10.3389/fmars.2014.00032>.
65. Biton E. 2020. Possible implications of sea level changes for species migration through the Suez Canal. *Sci Rep* 10. <https://doi.org/10.1038/s41598-020-78313-2>.
66. Kim Y, Jeon J, Kwak MS, Kim GH, Koh IS, Rho M. 2018. Photosynthetic functions of *Synechococcus* in the ocean microbiomes of diverse salinity and seasons. *PLoS One* 13:e0190266. <https://doi.org/10.1371/journal.pone.0190266>.
67. Lipizer M, Partescano E, Rabitti A, Giorgetti A, Crise A. 2014. Qualified temperature, salinity and dissolved oxygen climatologies in a changing Adriatic Sea. *Ocean Sci* 10:771–797. <https://doi.org/10.5194/os-10-771-2014>.
68. Marsan DW. 2016. Adaptive mechanisms of an estuarine *Synechococcus* based on genomics, transcriptomics, and proteomics, pp. 30–47. ProQuest diss theses. University of Maryland, College Park, Ann Arbor, Maryland. <https://doi.org/10.13016/M2P79P>.
69. Moutin T, Thingstad TF, Van Wambeke F, Marie D, Slawyk G, Raimbault P, Claustre H. 2002. Does competition for nanomolar phosphate supply explain the predominance of the cyanobacterium *Synechococcus*? *Limnol Oceanogr* 47:1562–1567. <https://doi.org/10.4319/lo.2002.47.5.1562>.
70. Sunagawa S, Coelho LP, Chaffron S, Kultima JR, Labadie K, Salazar G, Djahanschiri B, Zeller G, Mende DR, Alberti A, Cornejo-Castillo FM, Costea P, Cruaud C, d'Ovidio F, Engelen S, Ferrera I, Gasol JM, Guidi L, Hildebrand F, Kokoszka F, Lepoivre C, Lima-Mendez G, Poulain J, Poulos BT, Royo-Llonch M, Sarmiento H, Vieira-Silva S, Dimier C, Picheral M, Searson S, Kandels-Lewis S, Bowler C, de Vargas C, Gorsky G, Grimsley N, Hingamp P, Iudicone D, Jaillon O, Not F, Ogata H, Pesant S, Speich S, Stemmann L, Sullivan MB, Weissenbach J, Wincker P, Karsenti E, Raes J, Acinas SG, Bork P. Tara Oceans coordinators. 2015. Structure and function of the global ocean microbiome. *Science* 348:1261359–1261359. <https://doi.org/10.1126/science.1261359>.
71. Pernice MC, Forn I, Gomes A, Lara E, Alonso-Sáez L, Arrieta JM, del Carmen Garcia F, Hernando-Morales V, MacKenzie R, Mestre M, Sintes E, Teira E, Valencia J, Varela MM, Vaqué D, Duarte CM, Gasol JM, Massana R. 2015. Global abundance of planktonic heterotrophic protists in the deep ocean. *ISME J* 9:782–792. <https://doi.org/10.1038/ismej.2014.168>.
72. Ten Hoopen P, Cochrane G. Micro B3 Consortium. 2014. Ocean Sampling Day handbook - version of June 2014. <https://github.com/MicroB3-IS/osd-analysis/wiki/Guide-to-OSD-2014-data>. Accessed 15 January 2017.
73. Bolger AM, Lohse M, Usadel B. 2014. Trimmomatic: a flexible trimmer for Illumina sequence data. *Bioinformatics* 30:2114–2120. <https://doi.org/10.1093/bioinformatics/btu170>.
74. Logares R, Sunagawa S, Salazar G, Cornejo-Castillo FM, Ferrera I, Sarmiento H, Hingamp P, Ogata H, de Vargas C, Lima-Mendez G, Raes J, Poulain J, Jaillon O, Wincker P, Kandels-Lewis S, Karsenti E, Bork P, Acinas SG. 2014. Metagenomic 16S rDNA Illumina tags are a powerful alternative to amplicon sequencing to explore diversity and structure of microbial communities. *Environ Microbiol* 16:2659–2671. <https://doi.org/10.1111/1462-2920.12250>.
75. Jain C, Rodriguez-R LM, Phillippy AM, Konstantinidis KT, Aluru S. 2018. High throughput ANI analysis of 90K prokaryotic genomes reveals clear species boundaries. *Nat Commun* 9:5114. <https://doi.org/10.1038/s41467-018-07641-9>.
76. Caro-Quintero A, Konstantinidis KT. 2012. Bacterial species may exist, metagenomics reveal. *Environ Microbiol* 14:347–355. <https://doi.org/10.1111/j.1462-2920.2011.02668.x>.
77. Altschul SF, Gish W, Miller W, Myers EW, Lipman DJ. 1990. Basic local alignment search tool. *J Mol Biol* 215:403–410. [https://doi.org/10.1016/S0022-2836\(05\)80360-2](https://doi.org/10.1016/S0022-2836(05)80360-2).
78. Camacho C, Coulouris G, Avagyan V, Ma N, Papadopoulos J, Bealer K, Madden TL. 2009. BLAST+: architecture and applications. *BMC Bioinformatics* 10:421. <https://doi.org/10.1186/1471-2105-10-421>.
79. Huson DH, Auch AF, Qi J, Schuster SC. 2007. MEGAN analysis of metagenomic data. *Genome Res* 17:377–386. <https://doi.org/10.1101/gr.5969107>.
80. Oksanen J, Blanchet FG, Kindt R, Legendre P, Minchin PR, O'Hara RB, Simpson GL, Solymos P, Stevens MHH, Wagner H. 2015. vegan: Community Ecology Package. 2.2–1. <http://cran.r-project.org>, <https://github.com/vegandevs/vegan>. Accessed 15 January 2017.
81. Maechler M, Peter R, Struyf A, Hubert M, Hornik K. 2013. cluster: cluster analysis basics and extensions. R package version 1.14.4. <http://www2.uaem.mx/r-mirror/web/packages/cluster/citation.html>. Accessed 15 January 2017.
82. Wickham H. 2009. ggplot2: elegant graphics for data analysis, pp. 327. Springer New York, NY.

83. Vault D, Le Gall F, Marie D, Guillou L, Partensky F. 2004. The Roscoff Culture Collection (RCC): a collection dedicated to marine picoplankton. *nova\_hedwigia* 79:49–70. <https://doi.org/10.1127/0029-5035/2004/0079-0049>.
84. Rippka R, Coursin T, Hess W, Lichtlé C, Scanlan DJ, Palinska KA, Itean I, Partensky F, Houmard J, Herdman M, Lichtle C, Scanlan DJ, Palinska KA, Itean I, Partensky F, Houmard J, Herdman M. 2000. *Prochlorococcus marinus* Chisholm et al. 1992 subsp. *pastoris* subsp. nov. strain PCC 9511, the first axenic chlorophyll a2/b2-containing cyanobacterium (Oxyphotobacteria). *Int J Syst Evol Microbiol* 50:1833–1847. <https://doi.org/10.1099/00207713-50-5-1833>.
85. Marie D, Brussaard CPD, Partensky F, Vault D. 1999. Flow cytometric analysis of phytoplankton, bacteria and viruses, p 1–15. *In* Robinson JP (ed), *Current protocols in cytometry*. John Wiley & Sons, New York, NY.
86. Bernard O, Rémond B. 2012. Validation of a simple model accounting for light and temperature effect on microalgal growth. *Bioresour Technol* 123:520–527. <https://doi.org/10.1016/j.biortech.2012.07.022>.
87. Ocean Sampling Day Consortium P. 2015. Registry of samples and environmental context from the Ocean Sampling Day 2014. PANGAEA. <https://doi.org/10.1594/PANGAEA.854419>. Accessed 15 January 2017.